Available online at www.sciencedirect.com
SCIENCE DIRECT®
Journal of Controlled Release 95 (2004) 197–207
journal of controlled release
www.elsevier.com/locate/jconrel

Effect of cellular uptake of gelatin nanoparticles on adhesion, morphology and cytoskeleton organisation of human fibroblasts

Ajay Kumar Gupta[a,*], Mona Gupta[b], Stephen J. Yarwood[b], Adam S.G. Curtis[a]

[a] *Centre for Cell Engineering, IBLS, Joseph Black Building, University of Glasgow, Glasgow G12 8QQ, Scotland, UK*
[b] *Division of Biochemistry and Molecular Biology, IBLS, Davidson Building, University of Glasgow, Glasgow G12 8QQ, Scotland, UK*

Received 15 September 2003; accepted 18 November 2003

Abstract

The aim of present study was to prepare nanometer sized particles of gelatin via water-in-oil microemulsion system for drug and gene delivery applications. In this study, cross-linked gelatin nanoparticles encapsulating a fluorescent marker molecule fluorescein isothiocyanate-dextran (FITC-Dex, Mol. Wt. 19.3kDa) have been prepared, characterized and their influence on human fibroblasts has been assessed in terms of cell adhesion, cytotoxicity, light microscopy, scanning electron microscopy (SEM), transmission electron microscopy (TEM) and observation of cytoskeleton organisation. Gelatin nanoparticles were prepared inside the aqueous cores of sodium bis(2-ethylhexyl) sulfosuccinate (AOT)/*n*-hexane reverse micelles. Transmission electron microscopy image showed that the particles are spherical in shape with size of 37 ± 0.84 nm diameter. The release of FITC-Dex from the nanoparticles in phosphate buffer saline (pH 7.4) is found to increase with time and about 80% of the encapsulated dye is released in 6 h. Cell adhesion studies with human fibroblasts have shown that gelatin nanoparticles do not affect the number of cells adhered to glass as compared to control cells with no particles. Standard cell viability assay demonstrated that cells incubated with gelatin nanoparticles remained more than 100% viable at concentration as high as 500 μg/ml. From SEM image, it was observed that the nanoparticles were internalised and the fibroblasts exhibited vacuoles in the cell body with cell membrane abnormalities. Endocytosis of nanoparticles was confirmed from TEM studies and it resulted in disruption of F-actin and β-tubulin cytoskeleton. These studies show that the gelatin nanoparticles prepared by water-in-oil microemulsion systems are endocytosed by the fibroblasts without being toxic to cells even at high concentration of nanoparticles.

Keywords: Nanoparticles; Gelatin; Drug delivery; Cytoskeleton; Cytotoxicity

1. Introduction

The main target of many pharmaceutical delivery systems is to deliver the drug directly to the specific cell types and is successful only when the drug through its delivery vehicle is internalised into cells [1,2]. Mammalian cells utilize a variety of strategies to internalise particles and solutes including pinocytosis and phagocytosis, collectively known as endocytosis [3]. However, event of endocytosis occurs by the reorganisation of cell cytoskeleton [4,5] as the cytoskeleton is an integrated network of microfilaments, intermediate filaments and microtubules, and

* Corresponding author. 3/2, 15 Southcroft Street, Glasgow G51 2DH Scotland, UK. Tel.: +44-141-425-1938; fax: +44-141-330-3730.
E-mail address: akgupta25@hotmail.com (A.K. Gupta).

0168-3659/$ - see front matter © 2004 Elsevier B.V. All rights reserved.
doi:10.1016/j.jconrel.2003.11.006

there are structural and functional interactions between the cytoskeletal components [6]. The actins are primarily distributed in the periphery of the cell and are involved in dynamic processes of the cell such as crawling and phagocytosis. The microtubules originate near the nucleus and are responsible for maintaining the shape and polarity of fibroblasts. Intermediate filaments contribute to the static part of the cytoskeleton. Every filamentous structure has its own family of motor proteins that is responsible for its specific function [4–6].

In recent years, the strategy of utilizing nanoparticles as a carrier system for cell specific targeting and delivery of drugs has gained an increased interest [7,8]. However, the biocompatibility of nanoparticles is very closely related to cell behaviour in contact with them and particularly to cell adhesion to their surface [9]. Surface characteristics of these materials, whether their topography, chemistry or surface energy play an important role in cell adhesion on biomaterials. The attachment, adhesion and spreading belong to the first phase of nanoparticles–cell interactions and the quality of this first phase will influence the cell's capacity to proliferate and to differentiate itself in the presence of particles [9]. It is well known that apoptosis occurs in anchorage-dependent cells that are not allowed to attach to solid substrates via integrin mediated process [10]. So those surfaces that have weak cell adhesive interactions with the cells promote apoptosis resulting in decrease in cell viability. Thus, the immediate goal of designing any delivery vehicle would be to provide a system that promotes maximal cell adhesion to biomaterial surfaces with minimal inflammatory cell response [11]. Recently, many polymeric materials with above characteristics have been developed and utilized for drug and gene delivery applications. These materials include polyethylene glycol (PEG), PEG-based hydrogels, polyacrylamide, dextran, polyvinyl alcohol, poly(lactic acid-co-glycolide), polyvinylpyrrolidone, etc. [11–14]. Gelatin is a natural macromolecule and has a number of advantages over other synthetic polymers that makes it a suitable material to be used as nanoparticle carrier. Biocompatibility and biodegradability of gelatin is well documented in the literature [15,16].

Numerous work has been done using gelatin as an efficient carrier system for drugs and proteins [15,17]. Most of these studies have been done using BSA as a model drug [17]. Nakaoka et al. used gelatin microspheres as immunological adjuvant to enhance both humoral and cellular responses to antigen [18]. Many researchers have used gelatin nanoparticles as gene delivery vehicle [19–21]. Leong et al. used gelatin-DNA nanosphere coacervate as gene delivery vehicle to express the CFTR-gene into human tracheal epithelial cells [19]. While Amimji et al used PEG-modified gelatin nanoparticles for intracellular uptake in BT/20 human breast cancer cells [20]. Despite being used as a suitable carrier system, almost no attention has been directed towards the response of cytoskeletal organisation and adhesion behaviour of cells when subjected to gelatin nanoparticles.

In this study, gelatin nanoparticles in narrow size range have been prepared inside the aqueous core of the reverse micelles formed by AOT/*n*-hexane (w/o microemulsion). A fluorescent marker molecule, fluorescein isothiocyanate dextran (FITC-Dex, Mw = 19.3 kDa) has been encapsulated in these nanoparticles and the particles are characterized by various physicochemical means such as size measurements, loading capacity and in vitro release behaviour in buffer. The influence of these nanoparticles on human dermal fibroblasts in vitro has been assessed, prior to use in vivo conditions, in terms of cell adhesion, cytotoxicity, light microscopy, scanning electron microscopy (SEM), fluorescent observation of cytoskeleton organization (F-actin and tubulin) and transmission electron microscopy (TEM).

2. Materials and methods

2.1. Materials

All the chemicals were of reagent grade and were used without further purification. Gelatin type A (from porcine skin), glutaraldehyde, (3-(4,5-dimethylthiazol-2-yl)-2,5-diphenyltetrazolium bromide) MTT, sodium bis(2-ethylhexyl sulphosuccinate) (AOT), *n*-hexane, FITC-Dex (Mw = 19.3 kDa), sodium dihydrogen phosphate, disodium hydrogen phosphate, methanol and acetone were obtained from Sigma, Poole, UK. Double distilled water was used for all the experiments.

2.2. Preparation of cross-linked gelatin nanoparticles

Gelatin nanoparticles were prepared inside the inner aqueous core of reverse micellar droplets formed by dissolving surfactant, AOT in *n*-hexane. AOT has an advantage over other surfactants that it can form reverse micelles in non-aqueous solvents without the addition of any co-surfactant [22]. To 50.0 ml of 0.03 M AOT in *n*-hexane solution, 800 μl of 0.05% w/v of gelatin aqueous solution was added. About 10 μl (1.0% v/v) of glutaraldehyde was added to this solution to cross-link the nanoparticles. For void gelatin nanoparticles 20 μl of water was added to this solution. The solution was vortexed for 2 min and was stirred overnight at room temperature. The solution was homogeneous and optically transparent. For preparation of FITC-Dex loaded gelatin nanoparticles, 20 μl of FITC-Dex solution (35.0 mg/ml in water) was added in place of water. FITC-Dex was used as a fluorescent marker molecule not only to study the loading efficiency of gelatin nanoparticles for macromolecules but also to determine the release behaviour of the macromolecules from the nanoparticles. The gelatin nanoparticles were then recovered from reverse micelles as follows. Briefly, the organic solvent, *n*-hexane was evaporated off in a rotary evaporator and the particles from remaining dry mass were recovered by precipitation in an excess of acetone–methanol mixture (9:1 ratio) followed by filtration through Whatman filter paper no. 41. The precipitate was washed three to four times with acetone–methanol mixture to remove excess of AOT, the surfactant. The particles were resuspended in water followed by dialysis using 12 kD cut-off dialysis membrane against double distilled water. The dialysis was done for 3 h at 4 °C with water changed every 30 min. The aqueous suspension of the nanoparticles was lyophilised immediately to obtain dry powder before characterization. Lyophilized powder was easily redispersable in aqueous buffer.

2.3. Calculation of entrapment efficiency (E%)

The entrapment efficiency of the FITC-Dex in nanoparticles was calculated as follows: A FITC-Dex encapsulating gelatin nanoparticle solution was filtered through a Millipore filter (UFP2THK24 (100 kD cut-off). Free FITC-Dex present in aqueous buffer passed through the filter leaving the FITC-Dex entrapped in nanoparticles above the membrane. After separation of nanoparticles from the aqueous buffer, the extract including the repeated washing was collected. To a 100 μl of this solution, 500 μl of phosphate buffer saline (PBS, pH 7.4) was added and the concentration of the FITC-Dex was measured spectrophotometrically at 493 nm using a Shimadzu UV-160A UV–visible recording spectrophotometer. The amount of FITC-Dex present was calculated from the standard curve of the drug. The total amount of FITC-Dex left in the aqueous extract was subtracted from the amount of FITC-Dex originally added in the reaction medium and the entrapment efficiency (*E*%) was measured from the ratio of the amount of FITC-Dex entrapped to the total amount of FITC-Dex added $\times 100$.

2.4. Transmission electron microscopy (TEM) studies

The average particle size, size distribution and morphology were examined using a Zeiss 902 transmission electron microscope at a voltage of 80 kV. The aqueous dispersion of the particles was drop-cast onto a carbon coated copper grid and grid was air dried at room temperature before loading into the microscope.

2.5. Release profile of FITC-Dex from nanoparticles

A known amount of lyophilized powder of gelatin nanoparticles loaded with FITC-Dex was dispersed in 10 ml of phosphate buffer saline (PBS, pH = 7.4) as the nanoparticles can be dispersed easily in aqueous solutions by simple agitation for 2–3 min. 200 μl of the solution was distributed in 27 eppendorf tubes and was kept at 37 °C. At a predetermined interval of time the solution was filtered through a Millipore filter (UFP2THK24 (100 kD cut-off)). Free FITC-Dex present in the aqueous solution as a result of release from the nanoparticles passed through the filter and its concentration was determined spectrophotometrically at $\lambda_{max} = 493$ nm.

2.6. Cell culture

Infinity™ telomerase-immortalized primary human fibroblasts (hTERT-BJ1, Clonetech Laboratories,

USA) were chosen for cell culture studies, as these fibroblasts are highly stable, fast growing and represent well defined internal cytoskeleton components. The fibroblasts were seeded onto 13-mm glass coverslips in a 24 well plate at a density of 1×10^4 cells per well for 24 h after which the growth medium was removed and replaced with the medium containing nanoparticles. For control experiments, medium with no particles was used. The medium used was 71% Dulbecco's modified Eagle's medium (DMEM) (Sigma, Dorset, U.K.), 17.5% Medium 199 (Sigma, Dorset, U.K.), 9% fetal calf serum (FCS) (Life Technologies Ltd., Paisley, U.K.), 1.6% 200 mM L-glutamine (Life Technologies Ltd., Paisley, U.K.), and 0.9% 100 mM sodium pyruvate (Life Technologies Ltd., Paisley, U.K.). The cells were incubated at 37 °C in a 5% CO_2 atmosphere.

2.7. Cell adhesion assay

The effect of nanoparticles on cell adhesion was determined with cell suspension incubated with or without nanoparticles. Fibroblasts (h-TERT BJ1) were expanded in monolayer tissue culture. The cells were detached using trypsin-EDTA solution and divided into two individual populations. Cells were seeded with or without nanoparticles at a concentration of 0.2 mg/ml for 24 h onto coverslips (13 mm diameter; in triplicate) at 37 °C in 5% CO_2. The cells were washed twice with PBS, fixed in 4% formaldehyde/PBS (15 min, 37 °C), washed with PBS again and finally stained for 2 min in 1.0% Coomassie blue in acetic acid/methanol mixture at room temperature. The triplicate cell populations of adherent cells were counted in three separate light fields under a microscope using an eyepiece with average normalized to control cell population. The stained samples were observed by light microscopy and digital images of the fibroblasts were captured using a Hamamatsu Argus 20 camera for image processing.

2.8. In vitro cell viability/cytotoxicity studies

The MTT (3-(4,5-dimethylthiazol-2-yl)-2,5-diphenyltetrazolium bromide) assay is a simple non-radioactive colorimetric assay to measure cell cytotoxicity, proliferation or viability. MTT is a yellow, water-soluble, tetrazolium salt. Metabolically active cells are able to convert this dye into a water-insoluble dark blue formazan by reductive cleavage of the tetrazolium ring [23]. Formazan crystals, then, can be dissolved in an organic solvent such as dimethylsulphoxide (DMSO) and quantified by measuring the absorbance of the solution at 550 nm, and the resultant value is related to the number of living cells. To determine cell cytotoxicity/viability, the cells were plated at a density of 1×10^4 cells/well in 96 well plate at 37 °C in 5% CO_2 atmosphere. After 24 h of culture, the medium in the well was replaced with the fresh medium containing nanoparticles of varying concentrations. After 24 h, 20 μl of MTT dye solution (5 mg/ml in phosphate buffer pH 7.4, MTT Sigma) was added to each well. After 4 h of incubation at 37 °C and 5% CO_2 for exponentially growing cells and 15 min for steady-state confluent cells, the medium was removed and formazan crystals were solubilized with 200 μl of DMSO and the solution was vigorously mixed to dissolve the reacted dye. The absorbance of each well was read on a microplate reader (DYNATECH MR7000 instruments) at 550 nm. The spectrophotometer was calibrated to zero absorbance using culture medium without cells. The relative cell viability (%) related to control wells containing cell culture medium without nanoparticles was calculated by $[A]_{test}/[A]_{control} \times 100$.

Where $[A]_{test}$ is the absorbance of the test sample and $[A]_{control}$ is the absorbance of control sample.

2.9. Scanning electron microscopy for cell morphology

The cells were fixed with 1.5% glutaraldehyde (Sigma) buffered in 0.1 M sodium cacodylate (Agar Scientific, Stansted Essex, England, U.K.) (4 °C, 1 h) after a 24-h incubation period to allow the viewing of individual cells. The cells were then post-fixed in 1% osmium tetroxide (Agar Scientific, Stansted Essex, England, U.K.) followed by 1% tannic acid (Agar Scientific, Stansted Essex, England, U.K.) as a mordant. Samples were dehydrated through a series of alcohol concentrations (20%, 30%, 40%, 50%, 60%, 70%) followed by further dehydration (90%, 96%, 100% and dry alcohol). The final dehydration was in hexamethyldisilazane (Sigma, Poole, U.K.), followed by air-drying. Once dry, the samples were sputter coated with gold before examination with a Phillips SEM 500 field emission scanning electron microscope at an accelerating voltage of 12 kV.

2.10. Immunofluorescence and cytoskeletal organisation observation

After 24 h of culture the cells with the nanoparticles along with controls were fixed in 4% formaldehyde/PBS, with 1% sucrose at 37 °C for 15 min, to allow the viewing of individual cells. When fixed, the samples were washed with PBS, and a permeabilizing buffer (10.3 g of sucrose, 0.292 g of NaCl, 0.06 g of MgCl2, 0.476 g of Hepes buffer, 0.5 ml of Triton X, in 100 ml of water, pH 7.2) was added at 4 °C for 5 min. The samples were then incubated at 37 °C for 5 min in 1% BSA/PBS. This was followed by the addition of anti-β tubulin primary antibody (1:100 in 1% BSA/PBS, Sigma, Poole, U.K.) for 1 h (37 °C). Simultaneously, rhodamine-conjugated phalloidin was added for the duration of this incubation (1:100 in 1% BSA/PBS, Molecular Probes, Eugene, OR). The samples were next washed in 0.5% Tween 20/PBS (5 min ×3). A secondary, biotin-conjugated antibody (1:50 in 1% BSA/PBS, monoclonal horse antimouse (IgG), Vector Laboratories, UK) was added for 1 h (37 °C) followed by washing. A FITC conjugated streptavidin tertiary antibody was added (1:50 in 1% BSA/PBS, Vector Laboratories, U.K.) at 4 °C for 30 min, and given a final wash.

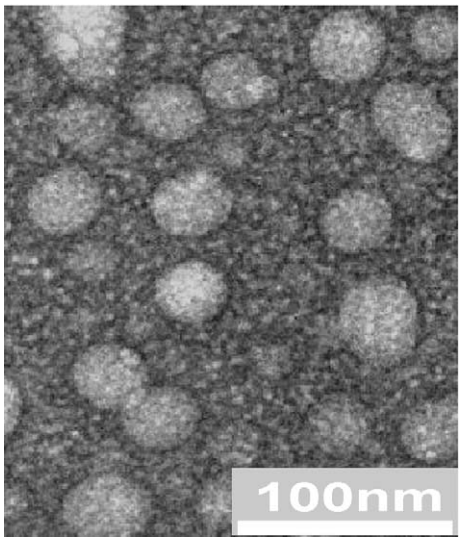

Fig. 1. Transmission electron microscopy picture of gelatin nanoparticles.

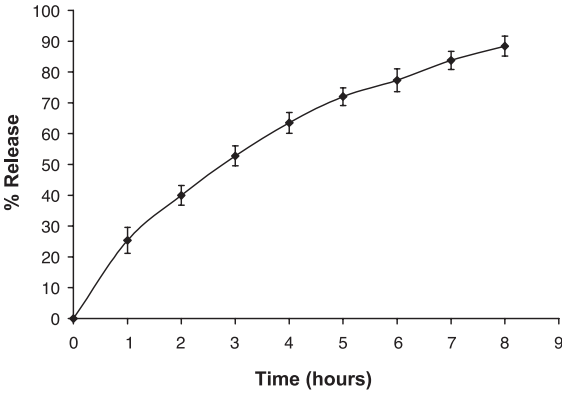

Fig. 2. Release profile of FITC-Dex from gelatin nanoparticles in PBS (results are represented as mean ± S.D.; $n = 3$).

Samples were mounted in Vectorshield fluorescent mountant (Vector Laboratories), and then viewed by fluorescence microscope (Vickers M17). The imaging system used was a Hamamatsu Argus 20 with an ×7 Hamamatsu CCD camera.

2.11. Transmission electron microscopy (TEM) studies

Cells were incubated with nanoparticle solutions for 24 h as before. Cells were fixed as for SEM, stained for 60 min with 1% osmium tetroxide and then taken directly through the alcohol steps up to dried absolute alcohol. The cells were finally treated with propylene oxide followed by 1:1 propylene oxide: resin for overnight to evaporate the propylene oxide. The cells were subsequently embedded in Spur's

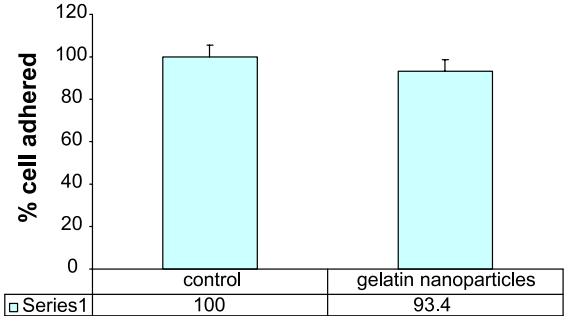

Fig. 3. Graphical representation of number of cells adhering to glass coverslips after 24 h at 37 °C (results are represented as mean ± S.D.; for $n = 3$, counted in triplicate in individual microscope fields).

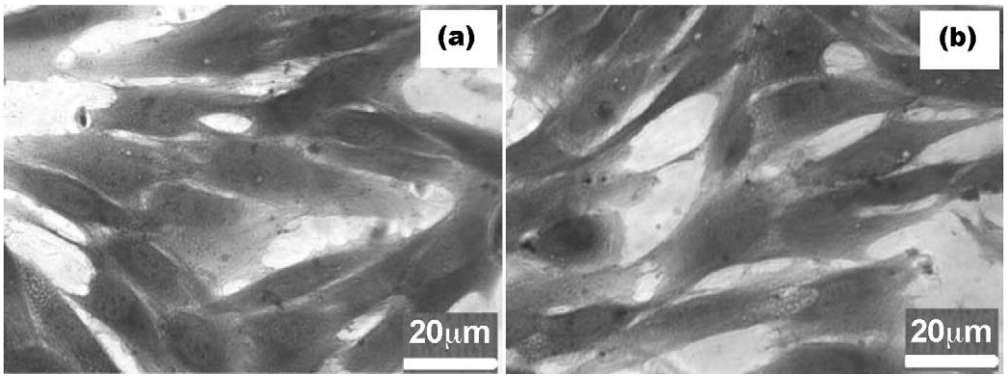

Fig. 4. Coomassie blue stained cells incubated for 24 h at 37 °C with (a) control and (b) gelatin nanoparticles ($n = 3$).

resin, and ultra-thin sections were cut and stained with lead nitrate and viewed under a Zeiss 902 electron microscope at 80 kV.

2.12. Statistical analysis

The statistical analysis of experimental data utilised the Student's *t*-test and the results were presented as mean ± S.D. Statistical significance was accepted at a level of $p < 0.05$.

3. Results

Cross-linked gelatin nanoparticles were prepared by using the highly monodispersed aqueous core of AOT/*n*-hexane reverse micellar droplets. Several TEM images of the particles were taken at magnification of 140,000. Average size of the particles was determined by measuring the size of around 200 particles. The particles as seen by TEM photographs were found to be monodispersed with narrow size distribution (Fig. 1). The particles were spherical in shape with average size of 37.0 ± 0.84 nm diameter. The entrapment efficiency of the nanoparticles for the FITC-Dex was found to be approximately 90%. The results from Fig. 2 showed that the release of the FITC-Dex from nanoparticles increased with increase in time with 80% of FITC-Dex released in 6 hours, while only 25% of the drug was released in initial 1 h.

The effect of nanoparticles on the adhesion of cells onto the glass surface was determined by counting the number of cells adhered to glass. Fig. 3 shows that the particles had no significant effect on the adhesion capacity of the cells compared to control cells (without particles). The general morphology of the fibroblasts incubated with nanoparticles after staining with Coommassie blue is shown in Fig. 4. The figure shows that the cells were well spread and there was no distinct change in morphology after 24 h incubation with gelatin nanoparticles relative to control cells.

The proliferation/viability of fibroblasts was measured by MTT assay after culturing for 24 h. The MTT assay for cell viability evaluation has been described as a very suitable method for detection of biomaterial toxicity [23]. The MTT assay relies on the mitochondrial activity of fibroblasts and represents a parameter

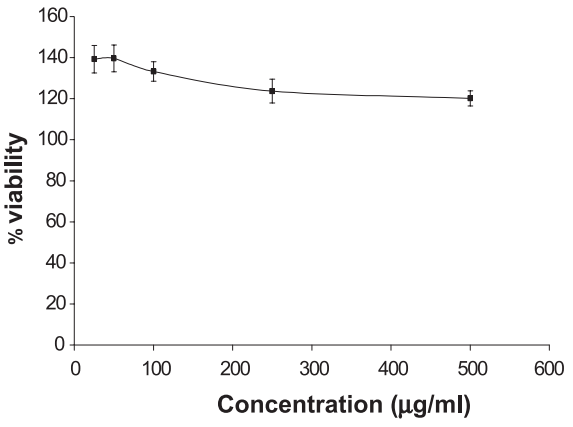

Fig. 5. Cytotoxicity profile of gelatin nanoparticles after 24 h incubation with human fibroblasts as determined by MTT assay. Percent viability of fibroblasts is expressed relative to control cells ($n = 6$).

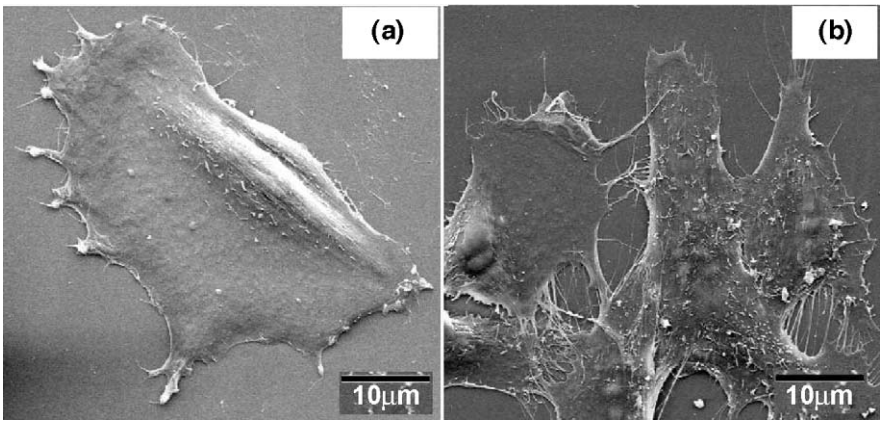

Fig. 6. SEM picture of human fibroblasts (a) control cells and (b) incubated with gelatin nanoparticles showing vacuoles.

for their metabolic activity. As it is evident from Fig. 5, the cytotoxicity of the nanoparticles increases in relation to increased concentration of gelatin. The gelatin nanoparticles were found to be more than 100% viable relative to control at the concentration as high as 500 μg/ml.

Scanning electron microscopy (SEM) images taken at 24 h provided further information on cell morphology in response to particle incubation. It was observed from the SEM results (Fig. 6) that the control cells are flat and well spread with small lamellapodia, suggesting cell motility. The control cells maintained their typical shape and surface morphology. Gelatin nanoparticles were found to be phagocytosed by the cells [24]. The fibroblasts exhibited vacuoles in the cell body with cell membrane abnormalities. In addition, cells stimulated the formation of many lamellapodia and filopodia that were observed projecting from the cell membranes over the glass surface.

Upon phagocytosis, the particles may affect the overall cytoskeleton of the cells by forming the vacuoles in the cell body, which may result in disrupted cytoskeleton and cell membrane protrusions [25]. From SEM results, we observed that the nanoparticles were phagocytosed into the cells [24]. For further information on the data obtained from above experi-

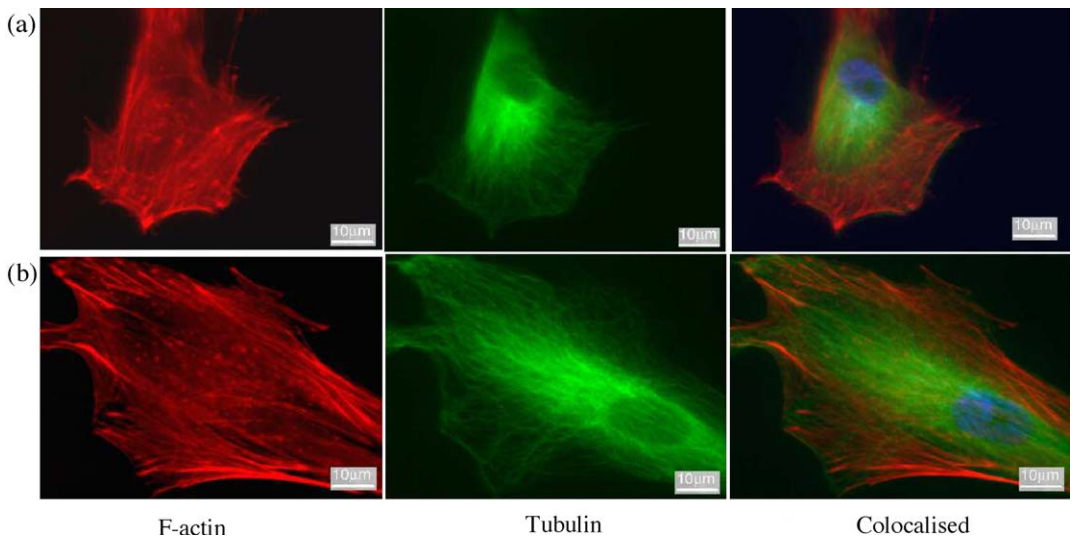

Fig. 7. Cells treated with (a) control and (b) gelatin nanoparticles and stained for tubulin (green), F-actin (red) and nucleus (blue) ($n = 3$).

ments, cytoskeletal dynamics was studied using immunofluorescent staining. Immunofluoroscent images (Fig. 7) were taken by staining for F-actin using rhodamine-phalloidin and for tubulin using anti-tubulin antibodies. The cells were also stained for cell nucleus using 4,6-diamidino-2-phenylindole (DAPI). In control cells, the microfilaments are well organized in thick bundles forming stress fibres. These fibres are stretched between cell surface and cytoplasm. The microtubules also form a dense network equally distributed around the nucleus in the whole cell volume. In the case of cells incubated with gelatin nanoparticles, the F-actin cytoskeleton appeared disrupted and disorganized. F-actin was organised in an anisotropic network with rather poorly formed filament bundles accumulated near the cell membrane region and in the lamellopodium and filopodium edges. It could also be seen in this case, that the β-tubulin were also disrupted and dispersed in some undefined regions of the cell.

To confirm that the particles were taken up by fibroblasts and also to determine the intracellular distribution of the gelatin nanoparticles in the fibroblasts, TEM of the cells was studied (Fig. 8). The TEM images showed that gelatin nanoparticles were taken up by fibroblasts. The cellular burden of the particles was often so great that much of the cell area was compromised of gelatin nanoparticles. The cytoplasm and nuclear membrane were intact. Several electron lucent voids containing gelatin nanoparticles were seen surrounded by several healthy appearing mitochondria. The nucleus of the cells also displayed numerous gelatin nanoparticles.

4. Discussion

The surfactant (for example AOT) when dissolved in non-polar solvents like hexane forms reverse micelles where hydrophobic tails of surfactants are assembled towards the bulk non-polar solvent and hydrophilic head is directed away from the bulk solvent inside enclosing a aqueous core [26]. The aqueous solution of gelatin and cross-linking agent was dissolved in this aqueous core of the reverse micelles and since these cores are hydrophilic, the cross-linking of gelatin and nanoparticle formation takes place inside these droplets. The size of the inner aqueous core of reverse micelles is in nanometer range so the gelatin nanoparticles prepared inside these nanoreactors have average size of 37.0 ± 0.84 nm diameter with spherical shape. The advantage of utilising this type of microemulsion system for nanoparticle formation is that the size of nanoparticles can be controlled by modulating the size of aqueous micellar core [27].

In order to obtain the stability of FITC-Dex loaded gelatin nanoparticles in the aqueous dispersion system, we have measured the release of FITC-Dex from nanoparticles in buffer solution. The percentage re-

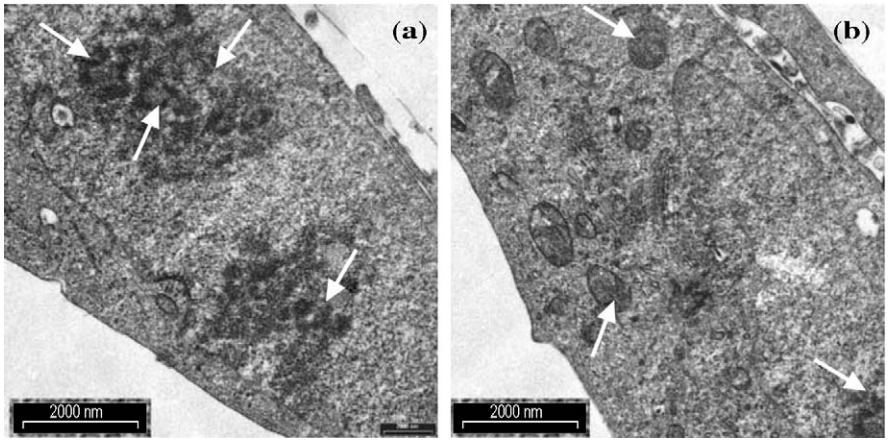

Fig. 8. TEM pictures of Human fibroblasts showing endocytosis of gelatin nanoparticles (a) and phagolysosomes (b) (see arrows). Some particles could be seen into nucleus of the fibroblasts (see arrows in lower right hand corner of figure (b)).

lease of the dye from the nanoparticles was found to increase with time. This is probably due to time dependent swelling of densely cross-linked gelatin matrix in aqueous solution and subsequent release of the macromolecules [28].

Gelatin is a hydrophilic polymer derived from collagen by hydrolytic extraction. It is highly soluble in hot water due to increased swelling of the matrix. The drug release kinetics from the gelatin nanoparticles depends on the rate of water uptake, drug dissolution/diffusion rate and the polymer glass-rubbery transition including matrix erosion/degradation rate [28]. At a higher temperature, the gelatin molecules have a higher mobility and lower degree of cross-linking, which increases the swelling degree of the hydrogel nanoparticles. Also the water content is affected by the degree of cross-linking of the gelatin matrix. Gelatin degradation by various cell types can occur either after phagocytosis or by extracellular protease acting at either neutral or acidic pH.

Toxicity of these nanoparticles was sufficiently low on human fibroblasts since no decrease in cell viability was observed in cells interacting with gelatin nanoparticles. It was observed from cell adhesion experiments that gelatin nanoparticles did not affect the adhesion of cells to glass as compared to control. The cells were healthy and maintained their morphology and adhesion capacity. It is known that cell adhesion is mediated by the interaction of surface proteins such as integrins with proteins in the extracellular matrix or on the surface of other cells or particles [29,30]. The phenomenon of cell adhesion is of crucial importance in governing a range of cellular functions including cell growth, migration, differentiation, survival and tissue organisation [29,30]. Thus the carrier system should not elicit a generic and chronic inflammatory response that can ultimately result in failure to achieve normal cell growth and function at the cell-particle surface.

Thus, using cytochemical staining and microscopic evaluation, we produced an estimate of the cytotoxicity of the particles. The cell viability can also be determined by proliferation assays using MTT. These methods give more quantitative graduations since the amount of MTT cleaved is directly proportion to the number of viable cells.

The SEM studies indicated that gelatin nanoparticles were endocytosed by the fibroblasts thereby forming vacuoles in the cell body. Cells were found to be well spread and stimulated the formation of many lamellipodia and filopodia that were observed projecting from cell membranes over the glass surface. Endocytosis of the particles resulted in disruption of the cell membrane and disorganised cell cytoskeleton. As the plasma membrane is directly linked to and functionally integrated with the underlying actin based cytoskeleton, it may be anticipated that endocytosis at the membrane would require the rearrangement of actin. Thus such a disrupted cytoskeleton is indicative of particle uptake [25,31]. It is well known that cytoskeleton reorganization, for example, the formation of lamellipodia, membrane ruffling and contraction of cells after particle internalisation, is required for cell proliferation, migration and in its metabolic actions [5]. Cytoskeleton reorganisation is controlled by small GTP-binding proteins such as Rho and Ras [6]. Rho is a small GTP-binding protein of the Rho family, a subset of the Ras superfamily [32]. Rho has been shown to regulate actin reorganisation induced by a wide range of extracellular factors in several adherent cell types [32]. In fibroblasts, it mediates the formation of stress fibres and focal adhesion induced by a variety of growth factors and by adhesion to fibronectin. Rho is also required for cell contractility. In fibroblasts and neuronal cells, lysophosphatidic acid (LPA)-induced contractility is prevented by the Rho inhibitor C3 transferase [33]. Ras is also a GTP-binding protein which is involved in membrane ruffling, pinocytosis [34] and the formation of stress fibres [35]. Ras protein is also critical for cytoskeleton reorganization such as the formation of ruffles [35].

The TEM studies indicate that a substantial number of particles were internalised confirming the above SEM and cytoskeletal organisation studies. The important finding of the present study was that there was no sign at the ultrastructural level of toxicity of gelatin nanoparticles over 24 hours. The ultrastructure of the cell organelles known to undergo degeneration in the presence of cytotoxic agents were basically normal despite the large number of particles present in the cytoplasm and nucleus. Little is known of how nanometer size polymeric particles may interfere with intracellular processes such as protein trafficking and if they more readily gain access to the blood circulation. The results of current study warrant further investigation in this regard.

5. Conclusions

This study shows that gelatin nanoparticles (of size less than 50nm diameter) prepared inside the aqueous cores of AOT/*n*-hexane reverse micelles are non-toxic to cells cultured at nanoparticles concentration up to 500 μg/ml. The electron microscopy and cytoskeleton organisation studies show that the particles could be internalised into the cells. The in vitro studies with human fibroblasts show that these nanoparticles could be used for efficient delivery of biopharmaceuticals into cells as well as for increasing drug delivery across cellular barriers. These studies, therefore, enable us to understand the interactions of gelatin nanoparticles with human fibroblasts in in vitro conditions in more details prior to use in in vivo situations. Further studies on the pharmacokinetics and toxicity of these nanoparticles in suitable in vivo models are being in progress.

Acknowledgements

The financial support of the European Commission Fifth Framework Growth Programme, grant number GRD5-CT2000-00375 and also the technical assistance of Mr. Eoin Robertson (Electron Microscopy Unit, IBLS, University of Glasgow, Glasgow, UK) is greatly appreciated.

References

[1] M. Hashida, M. Nishikawa, Y. Takakura, Receptor-mediated cell specific delivery of drugs to the liver and kidney, in: N. Ogata, S.W. Kim, J. Fiejen, T. Okano (Eds.), Advanced Biomaterials in Biomedical Engineering and Drug Delivery Systems, Springer-Verlag, Tokyo, Japan, 1996, pp. 86–90.
[2] R. Wattiaux, N. Laurent, S.W. Conninck, M. Jadot, Endosomes, lysosomes: their implications in gene transfer, Adv. Drug Deliv. Rev. 41 (2000) 201–208.
[3] H. Riezman, P.G. Woodman, G. van Meer, M. Marsh, Molecular mechanisms of endocytosis, Cell 91 (1997) 731–738.
[4] R. Gagesu, J. Gruenberg, E. Smyte, Membrane dynamics in endocytosis: structure–function relationship, Traffic 1 (2000) 84–88.
[5] T.J. Mitchison, L.P. Cramer, Actin-based cell motility and cell locomotion, Cell 84 (1996) 371–379.
[6] D. Bar-Sagi, J.R. Feramisco, Ras and Rho GTPases: a family reunion, Science 233 (1986) 1061–1068.
[7] S.M. Moghimi, A.C. Hunter, J.C. Murray, Long circulating and target specific nanoparticles: theory to practise, Pharm. Rev. 53 (2001) 283–318.
[8] P. Ramge, R.E. Unger, J.B. Oltrogge, D. Zenker, D. Begley, J. Kreuter, H. van Briesen, Polysorbate-80 coatings enhances uptake of polybutylcyanoacrylate (PBCA)-nanoparticles by human and bovine primary brain capillary endothelial cells, Eur. J. Neurol. 12 (2000) 1931–1934.
[9] N.J. Hallab, K.J. Bundy, K. O'Connor, R. Clark, R.L. Moses, Cell adhesion to biomaterials: correlations between surface charge, surface roughness, adsorbed protein and cell morphology, J. Long-Term Eff. Med. Implants 5 (3) (1995) 209–231.
[10] E. Ruoslahti, J.C. Reed, Anchorage dependence, integrins and apoptosis, Cell 77 (1994) 477–478.
[11] S.P. Massia, J. Stark, D.S. Letbetter, Surface immobilized dextran limits cell adhesion and spreading, Biomaterials 21 (2000) 2253–2261.
[12] E.W. Salzman, Polyethleneglycol oxide as a biomaterial, Am. J. Soc. Artif. Intern. Organs 6 (1983) 60–72.
[13] B.K. Brandley, R.L. Schnaar, Covalent attachment of an Arg-Gly-Asp sequence peptide to derivatizable polyacrylamide surfaces: support of fibroblast adhesion and long term growth, Anal. Biochem. 172 (1998) 270–278.
[14] A. Nakajima, Y. Hirano, M. Iida, Adsorption of plasma proteins on Arg-Gly-Asp-Ser peptide-immobilized poly(vinylalcohol) and ethylene-acrylic copolymer films, Polym. J. 22 (1990) 985.
[15] H.G. Schwick, K. Heide, Immunochemistry and immunology of collagen and gelatin, Bibl. Haematol. 3 (1969) 111–125.
[16] A.G. Ward, A. Courts, The Science and Technology of Gelatin, Academic Press, New York, 1977.
[17] K. Mladenovska, E.F. Kumbaradzi, G.M. Dodov, L. Makraduli, K. Goracinova, Biodegradation and drug release studies of BSA loaded gelatin microspheres, Int. J. Pharm. 242 (2002) 247–249.
[18] R. Nakaoka, Y. Tabata, Y. Ikada, Potentiality of gelatin microspheres as immunological adjuvant, Vaccine 13 (7) (1995) 653–661.
[19] V.L. Truong-Le, S.M. Walsh, W.B. Guggino, J.T. August, K.W. Leong, Gene transfer by DNA-Gelatin nanospheres, Arch. Biochem. Biophys. 361 (1) (1999) 47–56.
[20] G. Kaul, M. Amimji, Long Circulating Poly(ethyleneglycol)-modified gelatin nanoparticles for intracellular delivery, Pharm. Res. 19 (7) (2002) 1061–1067.
[21] V.L. Truong-Le, J.T. August, K.W. Leong, Gene delivery by DNA-Gelatin nanospheres, Hum. Gene Ther. 9 (1998) 1709–1717.
[22] Y.S. Leong, F. Candau, Inverse microemulsion polymerization, J. Phys. Chem. 86 (1982) 2269.
[23] T. Mosmann, Rapid colorimetric assay for cellular growth and survival: application to proliferation and cytotoxic assay, J. Immunol. Methods 95 (1993) 55–63.
[24] C.C. Berry, S. Wells, S. Charles, A.S.G. Curtis, Dextran and albumin derivatised iron oxide nanoparticles: influence on fibroblasts in vitro, Biomaterials 24 (25) (2003) 4551–4557.
[25] L.M. Fugimoto, R. Roth, J.E. Heuser, S.L. Schmid, Actin assembly plays a variable, but not obligatory role in recep-

tor-mediated endocytosis in mammalian cells, Traffic 1 (2000) 161–171.
[26] M.J. Hou, M. Kim, D.O. Shah, A light scattering study on the droplet size and interdroplet interaction in microemulsion of AOT-oil water systems, J. Colloid Interface Sci. 123 (1998) 398–412.
[27] N. Munshi, T.K. De, A.N. Maitra, Size modulation of polymeric nanoparticles under controlled dynamics of microemulsion droplets, J. Colloid Interface Sci. 190 (2) (1997) 387–391.
[28] C.S. Brazel, N.A. Peppas, Modelling of drug release from swellable polymers, Eur. J. Pharm. Biopharm. 49 (2000) 47–58.
[29] D.R. Absolom, W. Zingg, A.W. Neumann, Protein adsorption to polymer particles: role of surface properties, J. Biomed. Mater. Res. 21 (1987) 161–171.
[30] T.A. Haas, E.F. Plow, Integrin–ligand interactions: a year in review, Curr. Opin. Cell Biol. 6 (1994) 656–662.
[31] C. Lamazi, L.M. Fugimoto, H.L. Yin, S.L. Schmid, The actin cytoskeleton is required for receptor mediated endocytosis in mammalian cells, J. Biol. Chem. 33 (1997) 20332–20335.
[32] A. Hall, Small GTP-binding proteins and the regulation of the actin cytoskeleton, Annu. Rev. Cell Biol. 10 (1994) 31–54.
[33] M. Chrzanowska-Wodnicka, K. Burridge, Rho stimulated contractility drives the formation of stress fibres and focal adhesions, J. Cell Biol. 133 (1996) 1403–1415.
[34] D. Bar-Sagi, A. Hall, Induction of membrane ruffling and fluid-phase pinocytosis in quiescent fibroblasts by Ras proteins, Cell 103 (2000) 227–238.
[35] A.J. Ridley, A. Hall, The small GTP-binding protein Rho regulates the assembly of focal adhesions and actin stress fibres in response to growth factors, Cell 70 (1992) 389–399.